Peripheral and central inputs shape network dynamics in the developing visual cortex in vivo

Current Biology 22, 253–258, February 7, 2012 ©2012 Elsevier Ltd All rights reserved DOI 10.1016/j.cub.2011.12.026

Report

Peripheral and Central Inputs Shape Network Dynamics in the Developing Visual Cortex In Vivo

Friederike Siegel,[1,4,5] J. Alexander Heimel,[2] Judith Peters,[3] and Christian Lohmann[1,4,*]
[1]Department of Synapse and Network Development
[2]Department of Molecular Visual Plasticity
[3]Department of Neuroimaging and Neuromodeling
Netherlands Institute for Neuroscience, 1105 BA Amsterdam, The Netherlands
[4]Department of Cellular and Systems Neurobiology, Max Planck Institute of Neurobiology, 82152 Martinsried, Germany

Summary

Spontaneous network activity constitutes a central theme during the development of neuronal circuitry [1, 2]. Before the onset of vision, retinal neurons generate waves of spontaneous activity that are relayed along the ascending visual pathway [3, 4] and shape activity patterns in these regions [5, 6]. The spatiotemporal nature of retinal waves is required to establish precise functional maps in higher visual areas, and their disruption results in enlarged axonal projection areas (e.g., [7–10]). However, how retinal inputs shape network dynamics in the visual cortex on the cellular level is unknown. Using in vivo two-photon calcium imaging, we identified two independently occurring patterns of network activity in the mouse primary visual cortex (V1) before and at the onset of vision. Acute manipulations of spontaneous retinal activity revealed that one type of network activity largely originated in the retina and was characterized by low synchronicity (L-) events. In addition, we identified a type of high synchronicity (H-) events that required gap junction signaling but were independent of retinal input. Moreover, the patterns differed in wave progression and developmental profile. Our data suggest that different activity patterns have complementary functions during the formation of synaptic circuits in the developing visual cortex.

Results

The Developing Cortex Generates Spontaneous Activity Patterns

In vivo two-photon calcium imaging after bolus loading [11] in the visual cortex of anesthetized neonatal mice before eye opening (P8–P10) revealed synchronous network events in the somata and neuropil of layer 2/3 (Figures 1A and 1B; see also Movie S1 available online). Although individual cortical cells were active during only a proportion of network events, nearly all cells showed spontaneous activation over the course of the experiment.

To examine the effects of anesthesia, we studied cortical network activity at various isoflurane concentrations (low isoflurane: 0.7%–1%; high isoflurane: 1.5%) as well as in unanesthetized animals. Consistent with previous observations [12, 13], the frequency of spontaneous network events decreased with increasing levels of isoflurane (Figure 1C). However, other key parameters were unaffected by anesthesia (0.7%–1% isoflurane) compared to unanesthetized animals. The percentage of coactive cells per network event (participation rate) did not differ between anesthetized (62% ± 4%) and unanesthetized animals (57% ± 4%; n = 4 animals; $p > 0.05$; see also Figure 1D). Furthermore, neither the mean amplitude of the cellular calcium signal (Figure 1E) nor the variation in onset of activation in individual cells (jitter, Figure 1F) was affected by low isoflurane levels. Therefore, all subsequent recordings were performed under light anesthesia (0.7%–1%).

Manipulation of Retinal Inputs Affects Specifically Low, But Not High, Participation Rate Network Events

To investigate the origin of cortical network events, we manipulated peripheral activity arising from the retina and studied the effects on activity patterns in the visual cortex. First, we removed all retinal inputs by means of acute binocular enucleation and monitored the same population of cortical cells before and after enucleation (Figure S1A). The frequency of cortical network events decreased significantly after binocular enucleation (baseline: 1.6 ± 0.3 events/min; enucleation: 1.0 ± 0.2 events/min; n = 6 animals; $p < 0.05$; Figure S1B), and the remaining network events were characterized by significantly higher participation rates than during baseline recordings (baseline: 62% ± 3%; enucleation: 73% ± 4%; n = 6 animals; $p < 0.05$). More specifically, the frequency of network events with low to medium participation rates (20%–80%) was significantly reduced (Figures 2A and 2B); however, the remaining low to medium participation rate events did not differ in amplitude (baseline: 1.13 ± 0.03 F/F_0; enucleation: 1.15 ± 0.01 F/F_0), jitter (baseline: 0.5 ± 0.1 s; enucleation: 0.5 ± 0.1 s) or participation rate (baseline: 47% ± 1%; enucleation: 49% ± 3%; n = 6 animals). Interestingly, the frequency of high participation rate events (>80%) was unaffected by enucleation.

Next we augmented retinal activity pharmacologically by acute binocular injections of the water-soluble forskolin analog NKH477 [3]. This drug increases the activity of the enzyme adenylyl cyclase, which in turn elevates cyclic AMP levels [14] and increases the frequency of stage II retinal waves [15, 16]. After recording baseline activity, NKH477 (10 mM) or a control solution (0.9% saline) was injected into both eyes (~0.75 μl). After NKH477 application, the frequency of cortical network events increased significantly (baseline: 0.9 ± 0.1 events/min; NKH477: 1.4 ± 0.3 events/min; n = 11 animals; $p < 0.05$; Figure 2C; Figures S1C and S1D). The effect of NKH477 injections on cortical network dynamics was age-dependent because it affected P8 and P9, but not P10 animals (Figure 2D). This was most likely due to the specific action of NKH477 on cholinergic (stage II) retinal waves, which are less pronounced in older animals when glutamate signaling is required [16]. Therefore, we confined further analyses to P8 and P9 animals. Whereas the overall frequency of network events increased after NKH477 injections, the mean participation rate dropped (control: 65% ± 5%; NKH477: 54% ± 5%; n = 7 animals; $p < 0.05$). Specifically, the frequency of events

[5]Present address: Deutsches Zentrum für Neurodegenerative Erkrankungen, 53175 Bonn, Germany
*Correspondence: c.lohmann@nin.knaw.nl

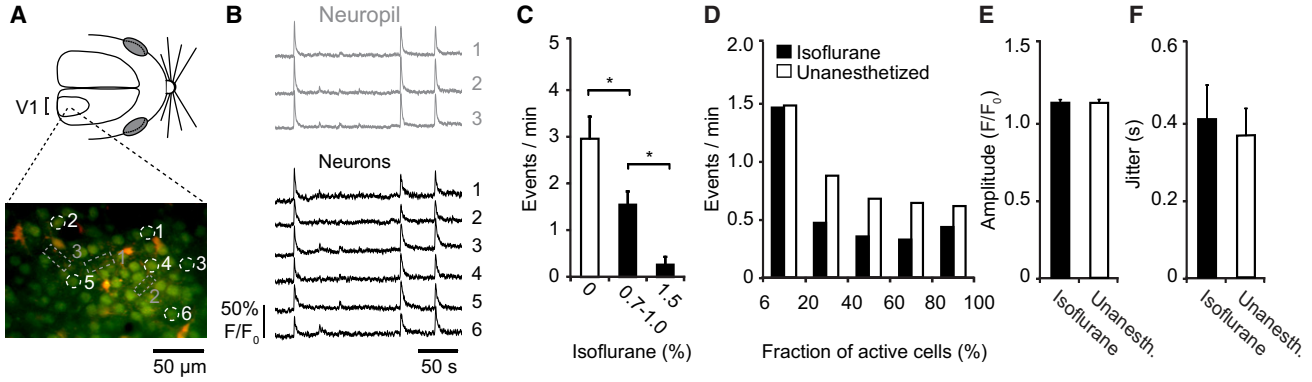

Figure 1. Network Events in the Developing Visual Cortex Show Similar Properties in Anesthetized and Unanesthetized Mice before Eye Opening

(A) Top shows schematic of the neonatal mouse and location of the primary visual cortex (V1). Bottom shows layer 2/3 cells in the visual cortex of a P10 animal labeled with OGB-1 (green). Astrocytes were specifically labeled by SR101 (red).

(B) Example traces of spontaneous network dynamics in the neuropil (gray traces) and in neurons (black traces) numbered in (A).

(C) Effects of isoflurane levels on the frequency of spontaneous network events (white bar: unanesthetized; black bars: anesthetized; *p < 0.05).

(D) Occurrence of network events with different participation rates (fraction of active cells) in isoflurane anesthetized (black bars) and unanesthetized animals (white bars).

(E and F) Basic characteristics of cortical network activity such as amplitude (E) and jitter (F) were not changed by isoflurane anesthesia. In (C), (E), and (F), data are represented as mean +SEM.

with low to medium participation increased after NKH477 application, whereas the frequency of events with high participation remained unchanged (Figures 2C and 2D). Saline injections affected neither frequency (baseline: 1.38 ± 0.25 events/min; saline: 1.18 ± 0.26 events/min; n = 5 animals; p > 0.05) nor participation rate (62% ± 5%; saline: 65% ± 4%; n = 5 animals; p > 0.05) of network events.

Taken together, the manipulations of retinal inputs suggested that two patterns of network activity coexisted in the developing visual cortex: low to intermediate participation rate events (20%–80%, L-events), which were largely triggered by retinal inputs, and high participation rate events (>80%, H-events), which were independent of retinal inputs.

L- and H-Events Represent Two Distinct Patterns of Spontaneous Network Activity In Vivo

We investigated the developmental profile of cortical network events and found that the frequency of cortical network events

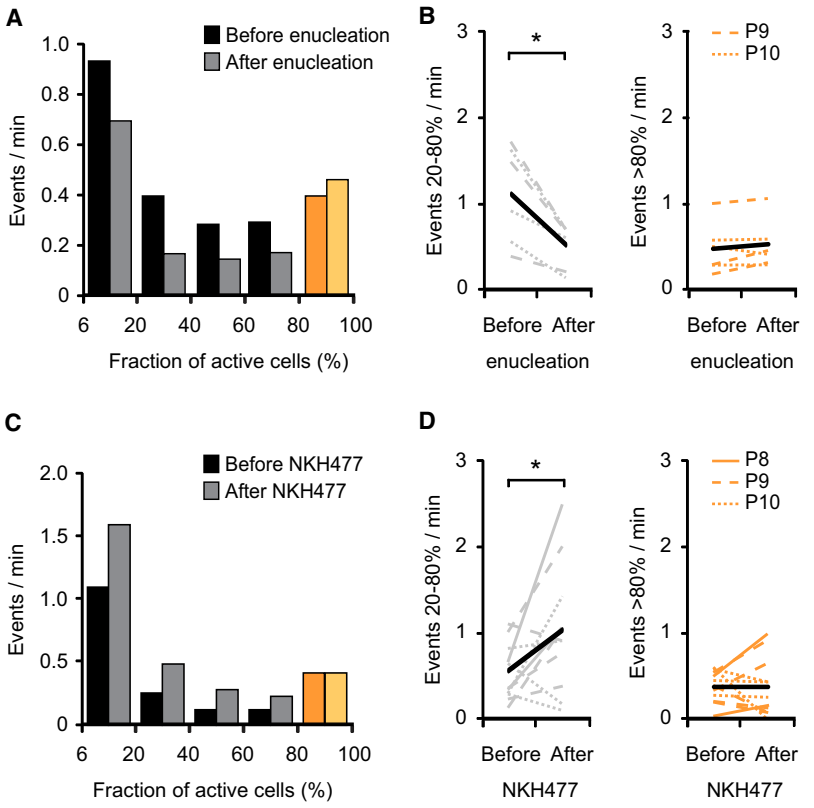

Figure 2. Manipulation of Retinal Inputs Differentially Affects Cortical Network Events

(A) Changes in participation rate after binocular enucleation (6%–80% participation: gray/black bars; >80% orange bars).

(B) Left shows that the mean frequency of cortical network events with low to medium participation rates (20%–80%, gray lines) was reduced after the removal of retinal inputs. Right shows that in contrast, the frequency of cortical events with high participation (>80%, orange lines) was not affected by enucleation (*p < 0.05; black lines represent means).

(C) Changes in participation rate after binocular injections of NKH477 (6%–80% participation: gray/black bars; >80% orange bars).

(D) The mean frequency of cortical network events with low to medium participation rates (20%–80%) was specifically increased after binocular NKH477 injections (gray lines), whereas the frequency of cortical events with high participation (>80%, orange lines) was unaffected by NKH477 (*p < 0.05).

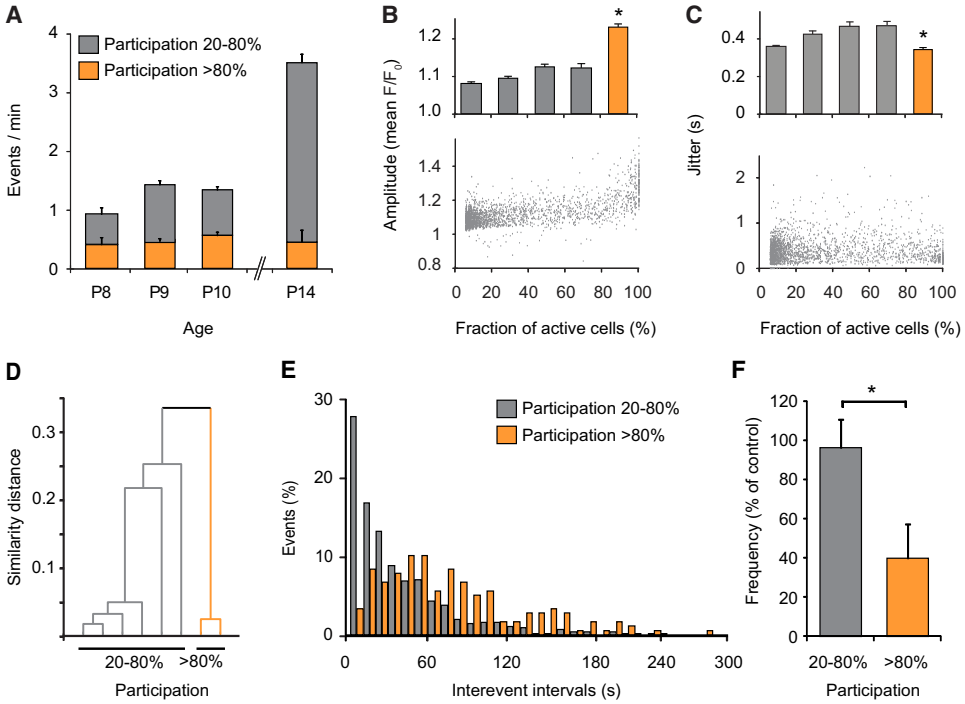

Figure 3. Characterization of Distinct Cortical Activity Patterns

(A) Frequency of spontaneous network events from P8 to P14. The frequency of L-events (20%–80%, gray bars) but not of H-events (>80%, orange bars) increased with age.

(B) Mean cellular amplitudes of cortical network events. Upper row shows quantification of the mean amplitudes for events with various participation rates (*$p < 10^{-38}$ compared to amplitudes at 20%–80%). Lower row shows scatterplot of the means of the peak cellular F/F_0 signal per network event.

(C) Temporal jitter of cortical network events. Upper row shows bar graph of the mean jitter for various participation rates. Lower row shows scatterplot of the cellular jitter for all network events (*$p < 10^{-8}$ compared to 20%–80%).

(D) Cluster analysis of network events grouped into 10% bins according to participation rate. The dendrogram represents Euclidian distances (y axis) in amplitude and jitter between network events of different participation rates. The clustering divides network events into two groups: 20%–80% (L-) and >80% (H-) events with some additional subclusters within the L-events group.

(E) Histograms of interevent intervals between events of the same type. The interevent intervals between L-events followed an exponential distribution, whereas the distribution of the interevent intervals between H-events showed a refractory period.

(F) The gap junction blocker carbenoxolone reduced the frequency of H-events significantly. L-events were not affected (*$p < 0.05$). In (A)–(C) and (F), data are represented as mean + SEM.

was not changed significantly between P8 and P10 but increased approximately 2.5-fold by the age of P14—around the time of eye opening (P14: 3.21 ± 0.41 events/min; n = 4 animals; $p < 0.05$; Figure 3A) in line with a previous study [17]. Whereas the frequency of L-events was specifically increased during that period, the frequency of H-events was not altered.

A detailed characterization of the two types of cortical network events in animals before eye opening (P8–P10) revealed that the mean amplitude over all coactive cells during network events was lower in L-events than in H-events (Figure 3B). Considering that calcium transients reflect the number of action potentials linearly [17], we estimate that firing rates during H-events were at least twice as high as during L-events. This suggested that individual cells get more and/or stronger inputs during H-events. The different types of cortical network events also differed in synchronicity: jitter, a measure for temporal variation of individual cellular activity during network activity, was higher (and hence synchronicity was lower) in L-events than in H-events (Figure 3C).

We investigated whether the classification of L- and H-events was supported independently of participation rate, solely by the parameters amplitude and jitter. Indeed, cluster analysis [18] based on amplitude and jitter between network events of different participation rates (in 10% bins) revealed the largest similarity distance between the 70%–80% and the 80%–90% bins (Figure 3D). Accordingly, the 20%–80% (L-events) and the >80% (H-events) groups differed highly significantly (Mann-Whitney test; $p < 10^{-6}$). Furthermore, a neuronal network was trained to cluster events according to jitter and amplitude, using the self-organizing map algorithm developed by Kohonen [19]. K-means clustering [20] of the trained map showed that L- and H-events were correctly assigned to the two different groups in 84% of the cases. These data demonstrate that L- and H-events can be quite cleanly (albeit not perfectly) separated by the 80% participation rate criterion.

The analysis of interevent intervals between two H-events showed a refractory period suggesting that H-events occurred in an oscillatory fashion (Figure 3E). In contrast, intervals between L-events followed an exponential distribution. This distribution pattern implies independence between two subsequent L-events, possibly because they are triggered independently at different sites (e.g., waves from each eye in binocular areas). L- and H-events occurred largely independently of each other (Figure S2).

Because H-events constituted a large proportion of all network events early during development, but not later, we

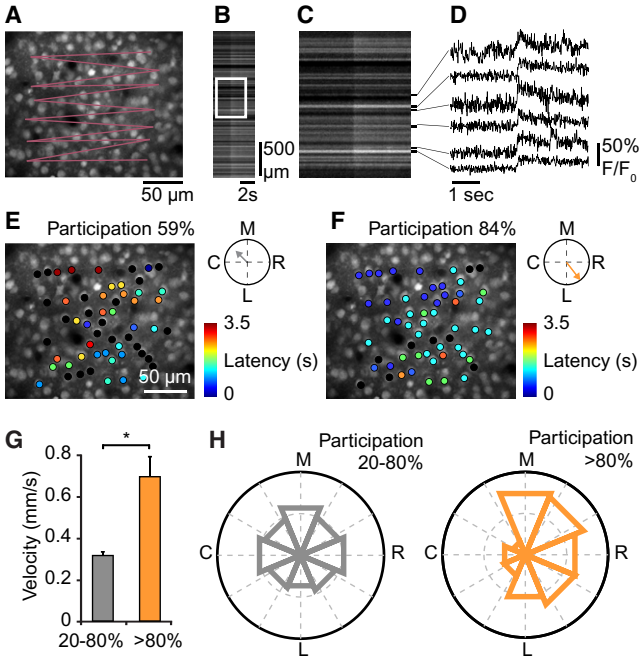

Figure 4. Spatiotemporal Fine Structure of Cortical Network Events

(A) Line-scan path overlay on top of OGB-1 labeled neurons.

(B) Line-scan across the entire line shown in (A) during one network event.

(C) Crop from (B) showing individual cells (bright lines).

(D) Traces of fluorescence changes in individual cells marked in (C).

(E) Sequential activation of individual neurons during a network event with intermediate participation (59%, L-event). The arrow indicates the direction and velocity of this wave (circle: 0.25 mm/s; M, medial; C, caudal; L, lateral; R, rostral). Individual cells are marked with colors, which denote the relative time points of their activation after the onset of activity in the first neuron (latency). Black dots mark neurons that are inactive during this event.

(F) Example of a network event with high participation rate (84%, H-event).

(G) The progression speed was faster in H- than in L-events. Data are represented as mean + SEM (*$p < 0.001$).

(H) Distribution of travel directions in L- (left) and H-events (right). H-events preferentially travel from caudal to rostral. The fraction of events in each direction is normalized to the fraction of shuffled events assigned to the same direction (the inner dashed circle is at 1).

investigated whether gap junctional coupling, which is required for early cortical network activity [21–23], may underlie H-event signaling. In fact, the acute cortical administration of the unspecific gap junction blocker carbenoxolone reduced the frequency of H-events significantly, but did not affect L-events (Figure 3F).

Finally, we studied the spatiotemporal patterns of network activation using line scans over many neurons with high temporal resolution (Figures 4A–4D, n = 6 animals). Many network events, independently of their participation rates, spread like waves across the cortex (Figures 4E and 4F; Figure S3). Although both L- and H-events progressed in waves, their progression velocity differed and was higher in H-events (Figures 4E–4G). In addition, the travel direction of waves differed between both patterns (chi-square test, $p < 0.05$; Figure 4H): L-events traveled more or less equally in all directions (chi-square test, $p = 0.6$), and H-events progressed preferentially from caudal to rostral (chi-square test, $p < 0.05$).

In summary, we find two distinct types of network activity that occur largely independently from each other. First, L-events recruit low to intermediate numbers of neurons and are generated largely in the retina, and their frequency increases with age. Second, H-events with high participation and synchronization are characterized by high amplitudes in all cells and fast wave kinetics. They are centrally generated, largely mediated by gap-junctional coupling, and constitute a major component of overall spontaneous activity in younger networks (P8–P10) but only a small fraction at later stages, around eye opening (P14).

Discussion

Spontaneous cortical network activity has been observed during the first 2 weeks of life in mice and rats. Field potential recordings revealed spindle bursts in the rat visual cortex before eye opening that occur at similar rates as the L-events described here (approximately three events per minute in unanesthetized animals), correlate with retinal waves and are strongly affected by manipulations of retinal activity [3]. This suggests that spindle bursts and L-events represent the same phenomenon. Previous in vivo calcium imaging studies revealed periodic network events that recruited many neurons in the visual and somatosensory cortex of neonatal mice [13, 17]. The frequency of these events increases strongly between P8–P10 and P14. Our analyses demonstrate that this increase in event frequency is entirely supported by L-events because the frequency of H-events showed a trend toward decreasing with age. Therefore, the differential development of both types of events will lead to an overall sparsification of network events, which has been observed for spontaneous activity in the developing cortex [13, 17].

By manipulating spontaneous retinal activity and recording cortical activity, we discovered that L- and H-events are triggered by different brain regions. The frequency of L-events is reduced after enucleation and strongly enhanced after stimulation of retinal waves with the forskolin analog NKH477, indicating that a significant proportion of L-events are triggered by retinal waves. This conclusion is further supported by the similarities in duration and frequency between L-events (duration: 1.6 ± 1.1 s, frequency: 2.4 ± 0.6 events/min) and retinal waves (duration: approximately 2 s; frequency 0.5–3 per minute; [24, 25]). However, after binocular enucleation, a proportion of L-events remain and exhibit identical participation rates, amplitude, and jitter values. This observation is reminiscent of previous studies in which spindle burst activity in sensory cortices persisted at reduced frequencies after deafferentiation [3, 26]. We consider it improbable that activity in the lateral geniculate nucleus (LGN) accounts for the L-events remaining after enucleation, because, in the ferret, deafferentiation of the thalamus from its retinal inputs causes the complete loss of activity in the LGN, which recovers only after about 50 min [6, 27]. A more likely possibility is that these L-events arise from nonvisual inputs to the visual cortex. For example, functional connections between cortical areas of different modalities [28, 29] may facilitate spread of network activity from other sensory systems into the visual cortex to elicit L-events independently of retinal inputs.

In contrast to L-events, H-events were unaffected by manipulations of retinal activity, demonstrating that they are independent of inputs from the peripheral visual system. Again, because retinal deafferentiation during development leaves the LGN essentially silent [6, 27], the thalamus is an unlikely source for H-events. In rat horizontal slices covering the entire rostrocaudal extension of the cortex, peripheral inputs are naturally absent and thus spontaneous activity, which travels

preferentially from caudal to rostral [30], might be constituted mostly or entirely of H-events. It has been suggested recently that spontaneous activity in the neonatal rodent cortex originates in the subplate [21] where neurons are highly interconnected via gap junctions [22]. Because H-events require gap junction signaling, they might be generated in the subplate.

What are the possible functions of L- and H-events during the development of the visual system? L-events increase in frequency just before eye opening, and the cellular contribution is relatively sparse resembling the activation patterns observed during visual stimulation after eye opening [31, 32]. Because retinal waves transmit information about the position and function of individual ganglion cells into the brain [25], waves could serve as "training patterns" that trigger cortical network events with spatiotemporal characteristics that enable correlation-based refinement of, for example, bottom-up or horizontal connections in relation to position in the visual field as well as orientation and direction tuning [33, 34]. In contrast to L-events, H-events do not show properties that render them good candidates for the activity-dependent refinement of connectivity. Information content is relatively low, because during each H-event virtually all cells in one area are coactive. Network activity, which is characterized by a high degree of correlation across individual cells, can cause homeostatic downregulation of synaptic weights [35]. Homeostatic mechanisms help neurons to maintain their activity levels in an optimal range. For example, a recent in vivo model of synaptic plasticity proposes that homeostatic control of synaptic strength is enforced by slow waves that occur during sleep, a specific form of synchronous network activity [36–38]. During development, local synaptic adaptations and global homeostasis may be interleaved: L-event activity may cause specific increases and decreases in strength of specific synapses, whereas H-events adapt overall synaptic strength to maintain firing rates within a certain range.

Supplemental Information

Supplemental Information includes three figures, Supplemental Experimental Procedures, and one movie and can be found with this article online at doi:10.1016/j.cub.2011.12.026.

Acknowledgments

We thank Volker Staiger and Martin Korte for animal monitoring software, Kenichi Ohki and Clay Reid for Matlab codes used for the analysis of cellular activity, and Max Sperling for support with the software controlling the two-photon microscope. In addition, we would like to thank Tobias Bonhoeffer for generous support and Helmut Kessels, Mark Hübener, and Juliette Cheyne for critically reading the manuscript. This work received additional support from the German Research Foundation (C.L.) and the Netherlands Organization for Scientific Research (C.L.).

Received: August 23, 2011
Revised: November 18, 2011
Accepted: December 9, 2011
Published online: January 19, 2012

References

1. Blankenship, A.G., and Feller, M.B. (2010). Mechanisms underlying spontaneous patterned activity in developing neural circuits. Nat. Rev. Neurosci. *11*, 18–29.
2. Khazipov, R., and Luhmann, H.J. (2006). Early patterns of electrical activity in the developing cerebral cortex of humans and rodents. Trends Neurosci. *29*, 414–418.
3. Hanganu, I.L., Ben-Ari, Y., and Khazipov, R. (2006). Retinal waves trigger spindle bursts in the neonatal rat visual cortex. J. Neurosci. *26*, 6728–6736.
4. Mooney, R., Penn, A.A., Gallego, R., and Shatz, C.J. (1996). Thalamic relay of spontaneous retinal activity prior to vision. Neuron *17*, 863–874.
5. Weliky, M., Kandler, K., Fitzpatrick, D., and Katz, L.C. (1995). Patterns of excitation and inhibition evoked by horizontal connections in visual cortex share a common relationship to orientation columns. Neuron *15*, 541–552.
6. Chiu, C., and Weliky, M. (2001). Spontaneous activity in developing ferret visual cortex in vivo. J. Neurosci. *21*, 8906–8914.
7. Grubb, M.S., Rossi, F.M., Changeux, J.P., and Thompson, I.D. (2003). Abnormal functional organization in the dorsal lateral geniculate nucleus of mice lacking the beta 2 subunit of the nicotinic acetylcholine receptor. Neuron *40*, 1161–1172.
8. Cang, J., Rentería, R.C., Kaneko, M., Liu, X., Copenhagen, D.R., and Stryker, M.P. (2005). Development of precise maps in visual cortex requires patterned spontaneous activity in the retina. Neuron *48*, 797–809.
9. Mrsic-Flogel, T.D., Hofer, S.B., Creutzfeldt, C., Cloëz-Tayarani, I., Changeux, J.P., Bonhoeffer, T., and Hübener, M. (2005). Altered map of visual space in the superior colliculus of mice lacking early retinal waves. J. Neurosci. *25*, 6921–6928.
10. Xu, H.P., Furman, M., Mineur, Y.S., Chen, H., King, S.L., Zenisek, D., Zhou, Z.J., Butts, D.A., Tian, N., Picciotto, M.R., and Crair, M.C. (2011). An instructive role for patterned spontaneous retinal activity in mouse visual map development. Neuron *70*, 1115–1127.
11. Stosiek, C., Garaschuk, O., Holthoff, K., and Konnerth, A. (2003). In vivo two-photon calcium imaging of neuronal networks. Proc. Natl. Acad. Sci. USA *100*, 7319–7324.
12. Greenberg, D.S., Houweling, A.R., and Kerr, J.N.D. (2008). Population imaging of ongoing neuronal activity in the visual cortex of awake rats. Nat. Neurosci. *11*, 749–751.
13. Golshani, P., Gonçalves, J.T., Khoshkhoo, S., Mostany, R., Smirnakis, S., and Portera-Cailliau, C. (2009). Internally mediated developmental desynchronization of neocortical network activity. J. Neurosci. *29*, 10890–10899.
14. Seamon, K.B., and Daly, J.W. (1986). Forskolin: its biological and chemical properties. Adv. Cyclic Nucleotide Protein Phosphorylation Res. *20*, 1–150.
15. Stellwagen, D., Shatz, C.J., and Feller, M.B. (1999). Dynamics of retinal waves are controlled by cyclic AMP. Neuron *24*, 673–685.
16. Huberman, A.D., Feller, M.B., and Chapman, B. (2008). Mechanisms underlying development of visual maps and receptive fields. Annu. Rev. Neurosci. *31*, 479–509.
17. Rochefort, N.L., Garaschuk, O., Milos, R.I., Narushima, M., Marandi, N., Pichler, B., Kovalchuk, Y., and Konnerth, A. (2009). Sparsification of neuronal activity in the visual cortex at eye-opening. Proc. Natl. Acad. Sci. USA *106*, 15049–15054.
18. Spath, H. (1980). Cluster Analysis Algorithms (Chichester: Ellis Horwood).
19. Kohonen, T. (1995). Self-Organizing Maps (Berlin: Springer).
20. MacQueen, J.B. (1967). Some Methods for Classification and Analysis of Multivariate Observations. In Proceedings of 5th Berkeley Symposium on Mathematical Statistics and Probability (Berkeley: California Press), pp. 281–297.
21. Hanganu, I.L., Okabe, A., Lessmann, V., and Luhmann, H.J. (2009). Cellular mechanisms of subplate-driven and cholinergic input-dependent network activity in the neonatal rat somatosensory cortex. Cereb. Cortex *19*, 89–105.
22. Dupont, E., Hanganu, I.L., Kilb, W., Hirsch, S., and Luhmann, H.J. (2006). Rapid developmental switch in the mechanisms driving early cortical columnar networks. Nature *439*, 79–83.
23. Yuste, R., Nelson, D.A., Rubin, W.W., and Katz, L.C. (1995). Neuronal domains in developing neocortex: mechanisms of coactivation. Neuron *14*, 7–17.
24. Demas, J., Eglen, S.J., and Wong, R.O.L. (2003). Developmental loss of synchronous spontaneous activity in the mouse retina is independent of visual experience. J. Neurosci. *23*, 2851–2860.
25. Stafford, B.K., Sher, A., Litke, A.M., and Feldheim, D.A. (2009). Spatial-temporal patterns of retinal waves underlying activity-dependent refinement of retinofugal projections. Neuron *64*, 200–212.

26. Khazipov, R., Sirota, A., Leinekugel, X., Holmes, G.L., Ben-Ari, Y., and Buzsáki, G. (2004). Early motor activity drives spindle bursts in the developing somatosensory cortex. Nature *432*, 758–761.
27. Weliky, M., and Katz, L.C. (1999). Correlational structure of spontaneous neuronal activity in the developing lateral geniculate nucleus in vivo. Science *285*, 599–604.
28. Frostig, R.D., Xiong, Y., Chen-Bee, C.H., Kvasnák, E., and Stehberg, J. (2008). Large-scale organization of rat sensorimotor cortex based on a motif of large activation spreads. J. Neurosci. *28*, 13274–13284.
29. Kayser, C., and Logothetis, N.K. (2007). Do early sensory cortices integrate cross-modal information? Brain Struct. Funct. *212*, 121–132.
30. Garaschuk, O., Linn, J., Eilers, J., and Konnerth, A. (2000). Large-scale oscillatory calcium waves in the immature cortex. Nat. Neurosci. *3*, 452–459.
31. Ohki, K., Chung, S., Ch'ng, Y.H., Kara, P., and Reid, R.C. (2005). Functional imaging with cellular resolution reveals precise micro-architecture in visual cortex. Nature *433*, 597–603.
32. Mrsic-Flogel, T.D., Hofer, S.B., Ohki, K., Reid, R.C., Bonhoeffer, T., and Hübener, M. (2007). Homeostatic regulation of eye-specific responses in visual cortex during ocular dominance plasticity. Neuron *54*, 961–972.
33. Ko, H., Hofer, S.B., Pichler, B., Buchanan, K.A., Sjöström, P.J., and Mrsic-Flogel, T.D. (2011). Functional specificity of local synaptic connections in neocortical networks. Nature *473*, 87–91.
34. Weliky, M., and Katz, L.C. (1997). Disruption of orientation tuning in visual cortex by artificially correlated neuronal activity. Nature *386*, 680–685.
35. Turrigiano, G.G., and Nelson, S.B. (2004). Homeostatic plasticity in the developing nervous system. Nat. Rev. Neurosci. *5*, 97–107.
36. Liu, Z.W., Faraguna, U., Cirelli, C., Tononi, G., and Gao, X.B. (2010). Direct evidence for wake-related increases and sleep-related decreases in synaptic strength in rodent cortex. J. Neurosci. *30*, 8671–8675.
37. Vyazovskiy, V.V., Cirelli, C., Pfister-Genskow, M., Faraguna, U., and Tononi, G. (2008). Molecular and electrophysiological evidence for net synaptic potentiation in wake and depression in sleep. Nat. Neurosci. *11*, 200–208.
38. Tononi, G., and Cirelli, C. (2006). Sleep function and synaptic homeostasis. Sleep Med. Rev. *10*, 49–62.